



Development of edible films based on reactive extrusion succinylated corn starch for the preservation of mango (*Mangifera indica* L. Cv. Kent)

Perla Rosa Fitch-Vargas¹ · Ernesto Aguilar-Palazuelos² · Xóchitl Ariadna Ruiz-Armenta² · Carlos Iván Delgado-Nieblas² · Claudia Barraza-Elenes² · Abraham Calderón-Castro²

Received: 14 October 2023 / Accepted: 14 January 2024 / Published online: 24 January 2024
© The Author(s), under exclusive licence to Springer Science+Business Media, LLC, part of Springer Nature 2024

Abstract

Growing concerns over synthetic plastic pollution have spurred interest in biodegradable food packaging. Starch edible films are an eco-friendly alternative that can enhance the shelf life of fruits and vegetables thanks to their excellent oxygen barrier properties. Nonetheless, Starch edible films have several disadvantages, such as low water resistance and poor mechanical properties. Modifying starch through reactive extrusion, particularly succinylation, offers a solution. Therefore, this research aims to prepare edible films using starch modified by succinylation with different safe-food-use degrees of substitution (DS, 0–0.05) through the extrusion process and Glycerol Content (GC, 15–30%). The succinylated starch edible films' (SSEF) functional properties and their effectiveness as a coating for mango preservation were evaluated. Results show that as the DS increased, SSEF had lower barrier properties and higher mechanical properties. Additionally, mangoes coated with SSEF exhibited better postharvest quality (weight loss, ΔE , firmness, pH, TA, and °Brix) than control fruit.

Keywords Edible Film · Succinylation · Extrusion process · Postharvest Quality

Introduction

Due to damage, about 25% of harvested fruits and vegetables are lost. Climacteric fruits, which comprise an essential part of tropical fruits, continue to ripen after harvest, making them more susceptible to damage and losses [1]. Various storage techniques have been developed to address this issue, slowing the ripening process of climacteric fruits and extending their shelf life [2]. In recent years, there has been a growing interest in developing and applying edible films (EFs) or coatings to preserve food quality and extend shelf life. This trend is driven by the need for more sustainable packaging alternatives and the benefits of using EFs, such as reducing food waste. Compared to traditional packaging materials, films and coatings made from edible materials offer advantages such as biodegradability, a lower carbon footprint, and no negative impact on human health. The functional properties of EFs vary depending on their composition, primarily determined by the matrix's plasticizer, polymer structure, and moisture content [3–5].

✉ Abraham Calderón-Castro
abcalcas@uas.edu.mx

Perla Rosa Fitch-Vargas
perlafitch@uas.edu.mx

Ernesto Aguilar-Palazuelos
eaguilar@uas.edu.mx

Xóchitl Ariadna Ruiz-Armenta
xochitlruiz@uas.edu.mx

Carlos Iván Delgado-Nieblas
cidelgadonieblas@uas.edu.mx

Claudia Barraza-Elenes
claudiabarraza@uas.edu.mx

¹ Facultad de Ciencias del Mar, Universidad Autónoma de Sinaloa, Paseo Claussen S/N, Col. Los Pinos, Mazatlán, Sinaloa 82000, México

² Posgrado en Ciencia y Tecnología de Alimentos, Universidad Autónoma de Sinaloa, Cd. Universitaria, Av. de las Américas y Josefa Ortiz S/N, Culiacán, Sinaloa 80200, México

Starch is widely recognized as one of the most commonly used ingredients in preparing EFs due to its low cost, abundance, and thermoplastic behavior. The amylose and amylopectin molecular weight determine the starch's functionality and their molecular organization within the granule. Researchers are exploring modified starches as potential materials for developing biodegradable products, including EFs, to expand the use of starch in food and industrial applications [6–8]. The hydroxyl groups of the starch polymer determine its chemical modification, which includes ether reactions, ester formation, oxidation, and hydrolysis. Chemical modification introduces functional groups that alter the physicochemical, functional, and structural properties of native starch, affecting paste formation, gelatinization, and retrogradation behavior [9]. Modified starches are classified into two categories based on their high and low degree of substitution (DS). The DS refers to the average number of hydroxyl groups substituted per glucose unit in starch. Since three hydroxyl groups are available per anhydroglucose unit, the maximum DS possible is three. Succinylation is a commonly used chemical modification method in the food industry that involves the reaction of alkenyl succinic anhydrides with granular starch in an aqueous suspension. The most commonly used reagent for this modification is succinic anhydride. Succinylated starches have hydrophobic and hydrophilic bifunctional groups, making them effective emulsifiers [6, 10, 11]. The Food and Drug Administration (FDA) recommends using succinylated starches with a DS of approximately 0.12, the equivalent of 4.0 g of succinic anhydride per 100 g of starch (dry basis), to ensure their safety in food applications [12, 13].

Conventional methods have been employed to generate modified starches with a low DS in aqueous conditions; however, they often require considerable amounts of water and chemicals [14]. In contrast, Calderón-Castro et al. [13] employed the extrusion process to obtain succinylated modified starches, highlighting advantages such as easy operation, low cost, high production capacity, and low solubility values. Previous studies have demonstrated that one of the primary drawbacks of EFs is

their hydrophilic character and poor mechanical behavior, which limits their application in food products stored under high humidity conditions [3, 15]. These disadvantages can be overcome by chemically modifying starch through succinylation, leading to EFs with improved functional properties [10, 12, 16]. Therefore, this study aimed to develop EFs using succinylated starch with different DS (under optimal processing conditions) and glycerol with good mechanical and barrier properties and evaluate their effectiveness as a coating on the postharvest quality of mango (*Mangifera indica* L. cv. Kent).

Materials and methods

Raw materials

Native corn starch (*Zea mays* L.) (Ingredion, Jalisco, Mexico) was employed for starch modification. Succinic anhydride (Sigma-Aldrich, St. Louis, MO, USA) was used to obtain the modified starches (MS). Glycerol was employed as a plasticizer (JT Baker®, Center Valley, USA).

Starch chemical modifications by reactive extrusion process

Table 1 shows the conditions for producing safe-food-use MS with different levels of succinylation. According to Calderón-Castro et al. [13], MS with safe-food-use DS were obtained using a twin-screw extruder (Model LT23L, Shandong Light M&E, China) with a 20:1 L/D ratio, 2:1 compression, and a 4 mm circular die. Using a hammer mill (Pulvex Model 200, Mexico City, Mexico), samples were grounded, sieved through a 200 µm mesh, and dried in an oven (Yamato DKN402C, CA, USA) at 60 °C for 12 h. The suspension was centrifuged for 10 min at 6000 rpm until it reached pH 5.0. The precipitate was washed, dried for 24 h at 45 °C, ground, and sieved with a 250 µm mesh. The resulting material was then packaged for further analysis and stored at 25 °C with a relative humidity of 53%.

Table 1 Predicted conditions to obtain the DS of the succinylated MS using the reactive extrusion

DS	Prediction conditions		
	ET (°C)	SS (rpm)	Reagents Concentration (%)
0	160	100	0
0.01	120	180	0.14
0.03	120	114	0.52
0.04	140	112	0.83
0.05	80	175	1.36

MS = modified starches, DS = Degree of Substitution, ET = Extrusion Temperature, SS = Screw Speed

Succinylated starch edible film preparation

The casting technique was used to produce the EFs according to the methodology described by Calderón-Castro et al. [15]. Table 2 shows the experimental design employed to produce the succinylated starch edible films.

(SSEF) with the safe-food-use degree substitution (DS) and Glycerol Content (GC) as the study factors. The thickness of SSEF was measured using a digital micrometer (Digital Insize, Model 3109-25 A, Spain), resulting in values of $50 \pm 5 \mu\text{m}$. Finally, SSEF were conditioned at a relative humidity (RH) of 53%.

Mechanical properties

Puncture strength (PS) and puncture deformation (D) of SSEF were assessed following the methodology described by Fitch-Vargas et al. [17], employing a universal texture analyzer (INSTRON 3342, Norwood, MA, USA). Twenty replicates were conducted per treatment.

Barrier properties

Water vapor permeability (WVP)

WVP was determined according to the methodology described by Fitch-Vargas et al. [17]. The SSEF were fixed on glass containers with 15 g of calcium chloride (JT Baker®, Center Valley, USA) and placed in a desiccator (Dry Keeper, Sanplatec Corp., Osaka, Japan) containing a saturated sodium chloride solution to maintain an RH of 75%. Over four days, the weight gained by the

calcium chloride was recorded every 12 h, with five replicates. WVP was calculated following Eq. (1):

$$WVP = \frac{MpxE}{Axtx\Delta p} \quad (1)$$

Where: Mp = absorbed moisture mass (g), E = thickness (m), A = exposed film area (m^2), t = time (s), and Δp = partial pressure difference through the film (Pa).

Carbon dioxide permeability (CO_2P)

The methodology described by Ayranci and Tunc [18] was used to determine the CO_2P of the SSEF. Glass containers were filled with four grams of ascarite and four grams of calcium chloride (CaCl_2). The SSEF were sealed with parafilm at the top of glass containers. The sealed glass containers were weighed and placed in a desiccator under a constant pressure of CO_2 (101324.71 Pa). Ascarite absorbed CO_2 , while CaCl_2 held the water produced by the chemical reaction. The weight increase of the glass containers was measured at intervals of 2 h for two days, with five replicates. The data was plotted against time, and a slope was calculated. By dividing the slope value by the total area of the EFs exposed to transmission, CO_2 transmission (CO_2T) was determined. Equation (2) was used to calculate CO_2P :

$$\text{CO}_2P = \frac{\text{CO}_2T}{p}xl \quad (2)$$

where p (101324.71 Pa) represents the pressure inside the desiccator and l is the SSEFs' average thickness.

Table 2 Experimental design and results of the response variables to obtain different combinations of DS and GC to prepare SSEF

Treatment	Factors		Response variables				
	DS	GC (%)	PS (N)	D (mm)	WVP (g m/ s m ² pa)	CO ₂ P (mL m /s m ² pa)	S (%)
1	0.01	17.20	13.14	8.40	2.92×10 ⁻¹¹	1.01×10 ⁻¹²	29.19
2	0.04	17.20	16.23	6.03	2.70×10 ⁻¹¹	2.21×10 ⁻¹³	22.50
3	0.01	27.80	7.29	13.40	5.63×10 ⁻¹¹	2.08×10 ⁻¹²	33.37
4	0.04	27.80	14.71	13.81	3.93×10 ⁻¹¹	1.16×10 ⁻¹²	22.46
5	0.00	22.50	8.97	15.34	4.15×10 ⁻¹¹	1.70×10 ⁻¹²	36.62
6	0.05	22.50	18.39	8.80	3.32×10 ⁻¹¹	1.84×10 ⁻¹³	18.15
7	0.03	15.00	15.49	4.64	2.50×10 ⁻¹¹	1.43×10 ⁻¹³	26.10
8	0.03	30.00	8.73	14.12	4.96×10 ⁻¹¹	1.98×10 ⁻¹²	29.20
9	0.03	22.50	12.80	13.74	3.84×10 ⁻¹¹	8.08×10 ⁻¹³	23.82
10	0.03	22.50	13.03	13.60	3.52×10 ⁻¹¹	5.35×10 ⁻¹³	26.23
11	0.03	22.50	12.26	13.27	3.42×10 ⁻¹¹	7.60×10 ⁻¹³	24.32
12	0.03	22.50	12.33	12.94	4.06×10 ⁻¹¹	9.17×10 ⁻¹³	27.00
13	0.03	22.50	12.27	12.17	3.84×10 ⁻¹¹	8.85×10 ⁻¹³	24.35

DS = Degree of Substitution; GC = Glycerol Content; PS = Puncture Strength; D = Deformation; WVP = Water Vapor Permeability; CO_2P = Carbon Dioxide Permeability; S = Water Solubility

Water solubility (S)

The S was determined as a percentage of disintegrated material according to the method described by Chiumarelli and Hubinger [19]. Five measurements per treatment were conducted. The S was calculated using Eq. (3)

$$\%S = \frac{(w_i - w_f)}{w_i} \times 100 \quad (3)$$

Where: %S = water solubility percentage, w_i = initial sample weight, and w_f = final sample weight.

Experimental design

A central composite rotatable model with $\alpha=1.41$ was employed, considering two numerical factors: safe-food-use degree of substitution (DS, 0–0.05) and Glycerol Content (GC, 15–30%). The assays were conducted randomly, as shown in Table 2. The factorial design comprised 13 experiments, which included four extreme data points at levels (−1) and (+1), four axial points located outside the factorial matrix but within the experimental range (−1.414 and +1.414), and a third set of five replicates at the center of the reference system (central points), coded as (0, 0). The significance of the factors in the model was assessed using the variance analysis (ANOVA) with a confidence level of 95%. The data analysis of the experimental design and the response surface graphs were carried out employing the Response Surface Methodology (RSM) with the Design Expert® Software Version 8 package (Stat-Ease, Inc., Minneapolis, USA). A second-order polynomial model (Eq. 4) was employed to predict the experimental behavior:

$$y_i = b_0 + b_1x_1 + b_2x_2 + b_1^2x_1^2 + b_2^2x_2^2 + b_1b_2x_1x_2 \quad (4)$$

Where: y_i = generic response; b_i = regression coefficients; x_1 = DS and x_2 = GC. The numerical optimization technique of the RSM was used to identify the optimal treatment conditions for DS (0–0.05) and GC (15–30%); the aim was to get SSEF with high PS values and low CO₂P, WVP, and S values. The optimized conditions were validated by triplicate. Statgraphics Plus 6.0 software assessed the significant difference between the predicted and experimental conditions. Native corn starch and succinylated modified starch and optimal treatment were characterized based on their microstructural properties (XRD and FT-IR) following the methodology reported by Calderón-Castro et al. [13]. Additionally, the optimal treatment was applied to evaluate the effect of SSEF on the postharvest quality of mango (*Mangifera indica* L.) cv. “Kent.”

Evaluation of postharvest quality characteristics

The 'Kent' cultivar's mature-green mango fruits (*Mangifera indica* L.) were meticulously harvested and sorted for uniformity, color, size, and absence of physical and microbial injuries and transported to the laboratory [20]. Mangoes were washed with a 100 ppm sodium hypochlorite solution and air-dried at room temperature. Fruits were randomly divided into three groups: Control (uncoated fruit), SSEF (fruit coated with SSEF), and CW (fruit coated with carnauba wax). The EFs were applied by immersing the entire fruit at $25 \pm 1^\circ\text{C}$, following the conditions employed in the packinghouse. Subsequently, the fruits were refrigerated at $12 \pm 1^\circ\text{C}$ with an RH of $90 \pm 5\%$ for 20 days. The following analyses were conducted to evaluate the effect of edible coatings on the postharvest quality of mangoes.

Physical analysis

Weight loss (WL) was assessed by measuring the difference in weight for 20 days and expressed as a percentage of the initial weight (%). To evaluate the fruit's firmness, a universal texture analyzer (INSTRON 3342, Norwood, MA, USA) fitted with an 11-mm-diameter probe was employed [15]. The pericarp was penetrated to a depth of 5 mm with a constant speed of 50 mm/min, and the results were reported in Newtons (N).

Chemical analysis

Following the AOAC [21] methodology, pH and titratable acidity (TA) were assessed. A 20 g sample was homogenized with 100 mL of distilled water employing an Ultra-Turrax (IKA T18 basic Ultra-Turrax, Germany) and filtered. The pH was measured employing a potentiometer (Orion Research Inc., Beverly, Mass., USA). TA was determined by titrating the homogenized solution with 0.1 N NaOH until reaching a pH of 8.1 ± 0.2 and expressed as a citric acid percentage. Using a refractometer (Atago, Fisher Scientific, Ga., USA), Total soluble solids (TSS) were determined and expressed as °Brix. Twelve slices were evaluated per replicate.

Statistical analysis

A completely randomized factorial experimental design was used to analyze the postharvest quality evaluation of mangoes. The factors were coating type and storage days at $12 \pm 1^\circ\text{C}$. The levels of A factor were Control, SSEF, and CW; meanwhile, the levels of B factor were 0, 4, 8, 12, 16, and 20 days. Per treatment, five replicates were performed in each experimental unit. Statistical data analyses were

performed through ANOVA using Statgraphics plus 6.0 (Manugistics, Rockville, MD), and the means were compared using the LSD test ($P \leq 0.05$).

Results and discussion

Functional properties of succinylated starch edible films (SSEF)

Puncture strength (PS)

Puncture strength (PS) is a widely studied parameter due to its impact on the performance of food products during transportation and storage. Strong films play a vital role in withstanding external forces and safeguarding the food's internal components. PS showed a significant regression model with values of $R^2_{adj} = 0.96$, $CV = 4.35\%$, P of $F < 0.01$, and did not show a lack of fit ($P > 0.05$), where the linear terms of DS and GC were significant ($P < 0.01$) (Table 3). The model for PS is presented in Eq. (5):

$$PS = +12.99 + 2.98DS - 2.32GC \quad (5)$$

Figure 1A shows the surface graph of the PS of SSEF. The PS increases when the GC is low (15%) and the DS is high (0.05). This combination results in resistant EFs with values of 18.39 ± 2.56 N. Zhong et al. [22] reported that even a minimal DS could result in films with high tensile strength. Ren et al. [23] found that succinic anhydride-modified starch films exhibited increased rigidity and resistance. Li et al. [5] suggested that self-aggregates forming within the modified polymer could explain the changes in the tensile strength of succinylated sweet potato starch films. Likewise, this effect could be attributed to the fact that the substituent groups hinder the reassociation of molecules with the native starch groups, thereby making the structure more resistant [24]. Furthermore, during starch succinylation, ester bonds are formed, which could act as cross-links between polymeric chains, reinforcing the material's molecular structure and improving its stiffness. Regarding the GC effect, it is well known that plasticizers weaken the intermolecular forces of starch; therefore, a lower GC could reduce the mobility

of the polymeric chains, resulting in increased material strength [25].

Deformation (D)

The D showed a significant regression model with $R^2_{adj} = 0.87$, $CV = 10.41\%$, and a P of $F < 0.01$ (Table 3). The linear term of DS and the linear and quadratic terms of GC were statistically significant ($P < 0.01$). The Eq. (6) shows the model for D:

$$D = +12.72 - 1.40DS + 3.27CG - 1.88CG^2 \quad (6)$$

The GC mainly affected the increase in D (Fig. 1B). The highest recorded value for D (15.34 ± 1.38 mm) was obtained with high GC (30%) and low DS (0). According to Dias et al. [26] plasticizers such as glycerol.

can disrupt hydrogen bonds between starch chains, increasing their mobility and D and decreasing their PS values. In addition, the increased DS resulted in a decrease in D values at low GC. The starch succinylation involves introducing succinyl groups into its structure, altering the molecular movement of polymeric chains, and limiting the material's ability to deform. Furthermore, this modification may increase the material's stiffness by forming cross-links between starch chains, thereby restricting the material's ability to elongate [27]. Nonetheless, as the GC increased at a DS of 0.05, there was an increase in D. This may be attributed to a plasticizing effect induced by the modified starch at these conditions. Similarly, Li et al. [5] reported that succinylated starch exhibited a plasticizing effect, forming self-aggregates of modified polymers that resulted in increased elongation in sweet potato starch-based EFs.

Barrier properties

Water vapor permeability (WVP)

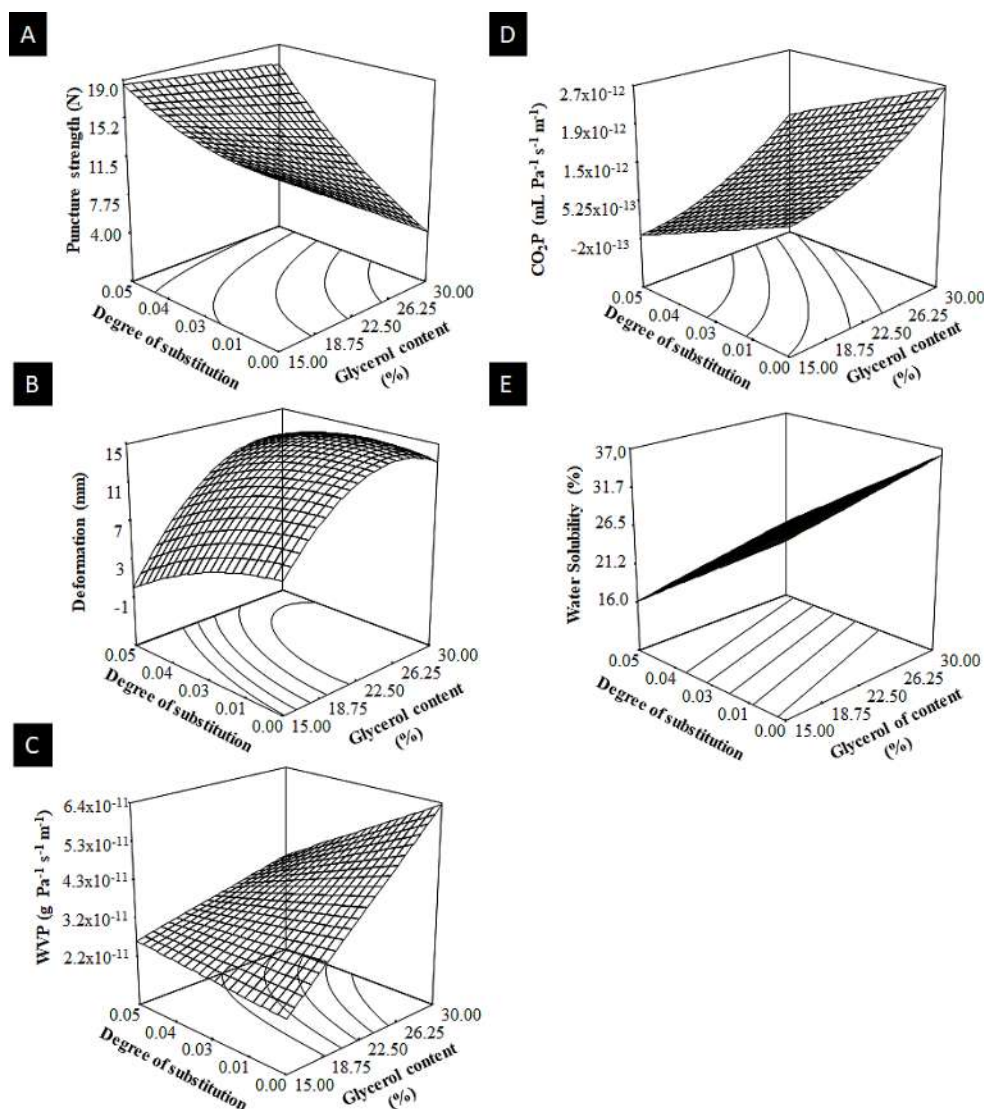
WVP showed a significant regression model with $R^2_{adj} = 0.94$, $CV = 5.45\%$, and a P of $F < 0.01$ (Table 3). The linear terms of the GC and DS were statistically significant ($P < 0.05$). The prediction model for WPV is presented in Eq. (7):

Table 3 Analysis of variance for the PS, D, WVP, and S responses in SSEF

Response	Adjusted R^2	CV (%)	F-Value	P of F	Lack of Fit
PS	0.96	4.35	92.68	< 0.01	0.1070
D	0.87	10.41	29.07	< 0.01	0.0556
WVP	0.94	5.45	68.46	< 0.01	0.8806
CO ₂ P	0.92	18.20	51.50	< 0.01	0.3358
S	0.85	7.09	35.35	< 0.01	0.2112

PS = Puncture Strength; D = Deformation; WVP = Water Vapor Permeability; CO₂P = Carbon Dioxide Permeability; S = Water Solubility

Fig. 1 Effect of DS and GC on the response variables of SSEF. Puncture Strength (A); Deformation (B); Water Vapor Permeability (C); Carbon Dioxide Permeability (D); Water Solubility (E)



$$WVP = +3.75 \times 10^{-11} - 3.85 \times 10^{-12} DS + 9.28 \times 10^{-12} GC \quad (7)$$

Figure 1C shows the WVP behavior regarding the DS and GC. The lowest WVP value ($2.50 \times 10^{-11} \pm 2.36 \times 10^{-12} \text{ g m Pa}^{-1} \text{ s}^{-1} \text{ m}^{-2}$) was obtained at lower GC (15%) and high DS (0.05). Regarding the effect of GC at different DS levels, it is observed that as it increases, there is a clear rise in WVP. It is well-established that glycerol can reduce the intermolecular interactions of the components of the thermoplastic matrix, generating a greater amount of free spaces and, therefore, higher WVP in EFs [28]. On the other hand, it is appreciated that increasing the level of succinylation leads to a decrease in WVP. A higher concentration of succinyl groups could enhance intermolecular interactions within the polymeric matrix, resulting in a denser film with improved barrier properties. Additionally, succinylation introduces hydrophobic groups into starch molecules and reduces the number of available hydroxyl groups to form

hydrogen bonds with water molecules, decreasing water affinity and permeability [11, 29]. Zhou et al. [30] reported that starch esterification by dodecenyl succinic anhydride decreased the availability of hydroxyl groups, leading to decreased water permeability and increased hydrophobicity of starch-based films. Similarly, Gahruie et al. [31] reported a decrease in the WVP of basil seed gum-based (BSG) films after OSA modification, mainly due to increased surface hydrophobicity.

Carbon dioxide permeability (CO_2P)

The CO_2P showed a significant regression model with $R^2_{adj} = 0.92$, $\text{CV} = 18.20\%$, and a P of $F < 0.01$ (Table 3). The linear term of the DS ($P < 0.01$) and the linear and quadratic terms of the GC ($P < 0.01$) significantly influenced the CO_2P . The quadratic model is shown in Eq. (8):

$$PCO_2 = +2.56 \times 10^{-12} - 3.65 \times 10^{-11} DS - 1.50 \times 10^{-13} GC + 3.48 \times 10^{-10} GC^2 \quad (8)$$

The surface graph in Fig. 1D shows the behavior of CO_2P regarding the DS and GC. It was observed that when the GC increased, the CO_2P increased significantly. Previous studies by Aguilar-Méndez et al. [32] and López et al. [33] reported that increased GC leads to higher gaseous permeabilities in starch-based films. This behavior could be attributed to the glycerol effect, which reduces intermolecular forces, increases free space in the polymeric matrix, and facilitates CO_2 diffusion through the film [34]. On the other hand, the CO_2P decreased when the DS increased. This phenomenon can be attributed to the succinyl groups, which improved intermolecular interactions due to their steric hindrance and electrostatic effects, resulting in a more compact film with decreased CO_2 permeability [27].

Water solubility (S)

Water solubility is a critical characteristic of EFs, mainly when the aim is to safeguard the package from water. A low S level is essential to ensuring the packaging material's integrity. The S showed a significant model of regression with $R^2_{adj} = 0.85$, $CV = 7.09\%$, and a P of $F < 0.01$, and did not show a lack of fit ($P > 0.05$). The linear terms of the DS and GC significantly ($P < 0.05$) influenced S. Equation (9) shows the model for S:

$$S = +26.41 - 5.46 DS + 1.60 GC \quad (9)$$

The behavior of the S regarding the DS and GC is shown in Fig. 1E. An increase in DS resulted in a decrease in S, obtaining minimum values of $18.15 \pm 1.84\%$. The introduction of succinyl groups into the starch structure gives it hydrophobic properties due to the presence of carbon atoms, limiting the intermolecular interactions between starch and water molecules. Furthermore, the chemical modification leads to a reduction in free hydroxyl groups, which also contributes to the decrease in water affinity and solubility of EFs [34]. According to Qiu et al. [27], the esterification of native starch by introducing carbonyl groups from succinic anhydride increases the hydrophobicity of the starch-based EFs. Gahruie et al. [31] observed decreased water solubility of BSG-based films after chemical modification with octenyl succinate anhydride, attributed to increased hydrophobicity.

On the other hand, the S increased with higher GC, indicating increased hydrophilicity. As a plasticizer, glycerol interacts with the polymeric matrix, creating additional spaces between the polymeric chains. These interactions facilitate water diffusion and enhance the material's capacity to absorb water, resulting in an increased solubility, as

reported by Cerqueira et al. [28]. According to Chiumarelli and Hubinger [19], the hydrophilic nature of glycerol significantly influences the S of starch-based films.

Numerical optimization

Numerical optimization was carried out to find the best values of DS and GC to obtain EF with the highest PS values and the lowest WVP, CO_2P , and S values. The optimum treatment for the SSEF was $DS = 0.05$ and $GC = 19.85\%$. With these optimal conditions, the following predicted values were obtained by each of the corresponding mathematical models: $PS = 18.39 \pm 1.06$ N, $WVP = 2.98 \times 10^{-11} \pm 3.19 \times 10^{-12}$ g m Pa^{-1} s $^{-1}$ m $^{-2}$, $CO_2P = 7.13 \times 10^{-14} \pm 8.33 \times 10^{-08}$ mL m Pa^{-1} s $^{-1}$ m $^{-2}$ and $S = 17.65 \pm 1.84\%$.

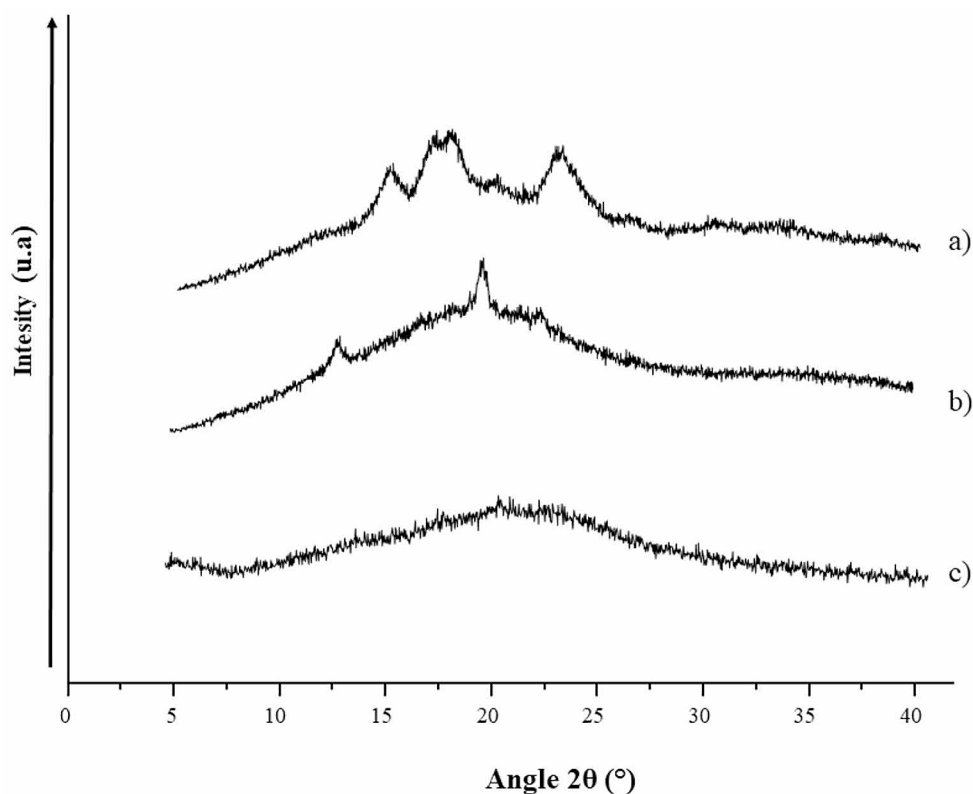
The SSEF was prepared under predicted optimum conditions to verify the models experimentally. The following values were obtained: $PS = 18.67 \pm 0.97$ N, $WVP = 3.34 \times 10^{-11} \pm 5.40 \times 10^{-12}$ g m Pa^{-1} s $^{-1}$ m $^{-2}$, $CO_2P = 6.75 \times 10^{-14} \pm 5.69 \times 10^{-08}$ mL m Pa^{-1} s $^{-1}$ m $^{-2}$, and $S = 18.30 \pm 2.51\%$. By comparing the experimental values with the predicted values by the mathematical models, no significant differences were observed among them ($P > 0.05$).

X-ray diffraction (XRD)

Figure 2 shows the X-ray diffractogram patterns of native corn starch, succinylated modified corn starch (SMS), and optimum SSEF. Corn starch showed an A-type crystallinity pattern, characteristic of cereals, with values 2θ of $\approx 17.94^\circ$ and $\approx 23.18^\circ$. SMS showed a principal peak at $\approx 19.76^\circ$ (2θ), exhibiting a VH-type crystallinity resulting from the processing at high temperatures in the reactive extrusion [35]. Likewise, native corn starch and SMS recorded a relative crystallinity (RC) of $16.5 \pm 2.12\%$ and $3.8 \pm 1.52\%$, respectively. The reduction in RC can be attributed to the reactive chemical modification process, which promoted the fragmentation of the native starch granules and subsequent esterification [17, 36]. Furthermore, SSEF exhibited an RC of $2.3 \pm 0.63\%$ with a large amorphous halo with low-intensity peaks regarding the native starch and SMS. This modification in the crystalline spectrum is attributed to the edible's film formation (casting technique), where the succinate starch granules had more significant fragmentation than raw material [4]. In addition, introducing octenyl succinyl groups to the starch molecule has been reported to decrease its ability to form crystals since these

groups generate a steric hindrance that compacts the starch molecules through hydrogen bonds during the film formation [11].

Fig. 2 XRD patterns of native starch (a), succinylated modified starch (b), and SSEF (c)



Infrared spectroscopy analysis (FT-IR)

Figure 3 shows the FT-IR spectra of native corn starch, SMS, and optimum SSEF. All samples recorded bands at $700\text{--}904\text{ cm}^{-1}$ (glycosidic bonds stretching vibration) and $3200\text{--}3600\text{ cm}^{-1}$ (O–H group) [37]. Regarding native corn starch, $1000\text{--}1225\text{ cm}^{-1}$ peaks correspond to C–O bond stretching, while bands at $1426\text{--}1864\text{ cm}^{-1}$ and $2740\text{--}2953\text{ cm}^{-1}$ are associated with absorbed water and C–H stretching vibration, respectively. On the SMS spectra, $1924\text{--}1510\text{ cm}^{-1}$ peaks are associated with C=O and C–O stretching vibrations [38]. Wang et al. [16] reported that peaks at $1573\text{--}1730\text{ cm}^{-1}$ indicate that the succinyl group was successfully esterified. Moreover, it was observed in SMS spectra that after the starch chemical modification, the intensity of some peaks was reduced due to the disruption of chemical bonds produced by the reactive extrusion process [4].

On the other hand, in the optimum SSEF were identified peaks at 2740 cm^{-1} , as well as 996, 1100, and 1180 cm^{-1} , corresponding to C–H stretching associated with anhydroglucose units of succinylated starch and C–O bond stretching, respectively [39, 40]. Peaks at $1600\text{--}1720\text{ cm}^{-1}$ were related to the stretching vibration of C=O and the formation of carbonyl ester groups [39]. These findings validate the presence of succinyl groups in the SSEF, which likely contribute to an increased number

of intermolecular interactions as hydrogen bonding and, consequently, improved physicochemical properties and stability.

Coated fruits quality evaluation

Weight loss (WL)

Figure 4a shows mango fruits' weight loss (WL) after 20 days of storage. WL increased over time for all three treatments due to natural maturation and fruit transpiration, leading to water loss. Control treatment exhibited the highest WL, recording $7.68 \pm 1.29\%$ on day 20. Control fruits showed significant differences ($P < 0.05$) regarding SSEF and CW on days 12, 16, and 20. This behavior suggests that applying EFs reduced the water vapor diffusion, reducing the WL. These materials can interact with the food surface, forming a semi-permeable membrane that prevents water loss [40]. Additionally, it is noteworthy that starch-based coatings, owing to their excellent cohesion, tend to reduce the diffusion of gases like oxygen, contributing to the regulation of metabolic processes such as fruit respiration and ripening [32, 41].

The WL of SSEF and CW after 20 days of storage was $5.03 \pm 0.89\%$ and $4.05 \pm 1.12\%$, respectively, without significant differences ($P > 0.05$) among them. It is well known that the hydrophobic nature of CW provides

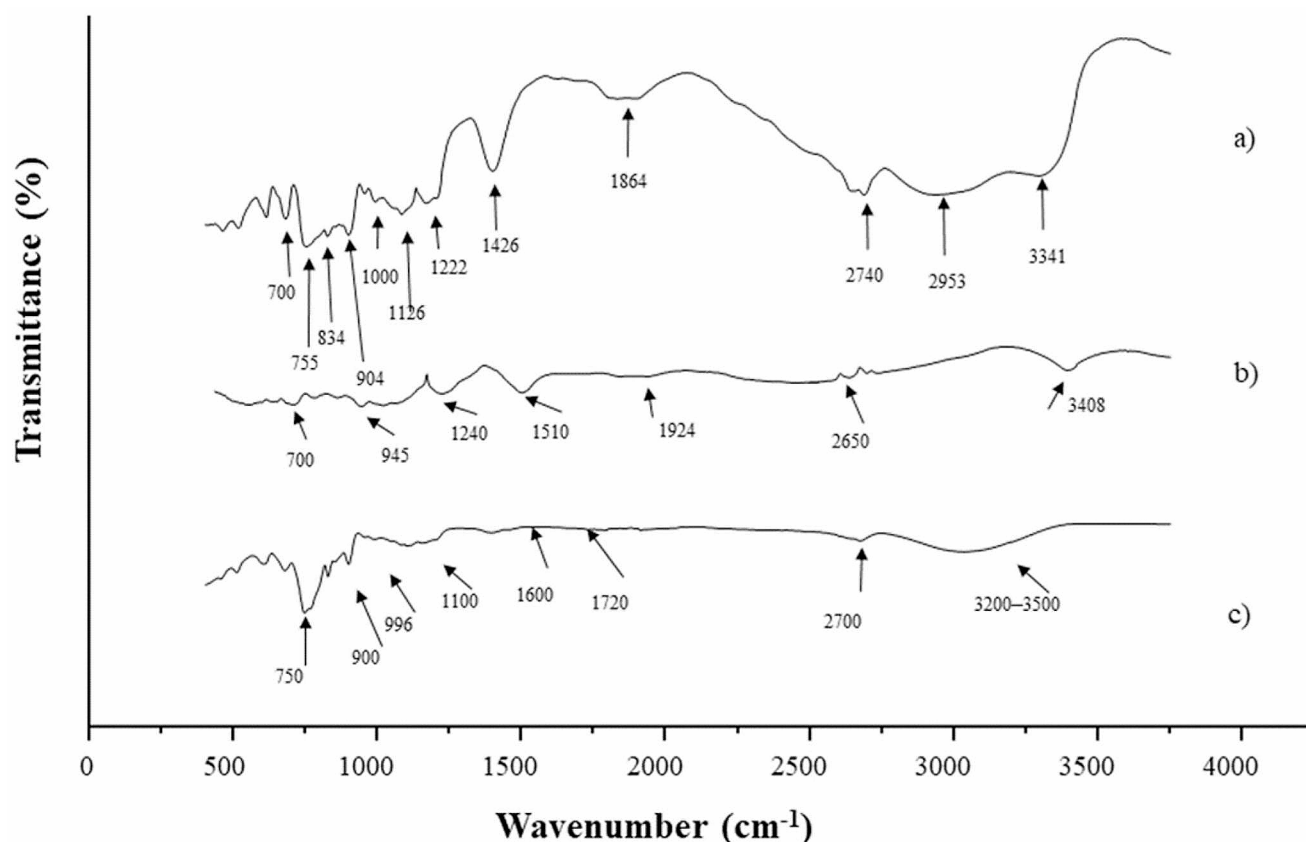


Fig. 3 FT-IR spectra of native starch (a), succinylated modified starch (b), and SSEF (c)

an effective barrier against water loss [15, 19]. Nonetheless, SSEF presented a similar behavior to CW due to the hydrophobicity provided by the succinyl groups, avoiding water vapor transmission [33]. Moreover, chemical interactions, such as hydrogen bonding, may have occurred between succinylated starch and the hydroxyl groups on mango surface components, promoting proper adhesion. Thus, the effective interaction between the coating and the fruit explains the prevention of water evaporation and WL [42, 43]. Punia et al. [9] reported that EFs based on wheat starch modified with octenyl succinic anhydride in grapes showed a reduction in WL, preventing shrinkage compared to uncoated fruits.

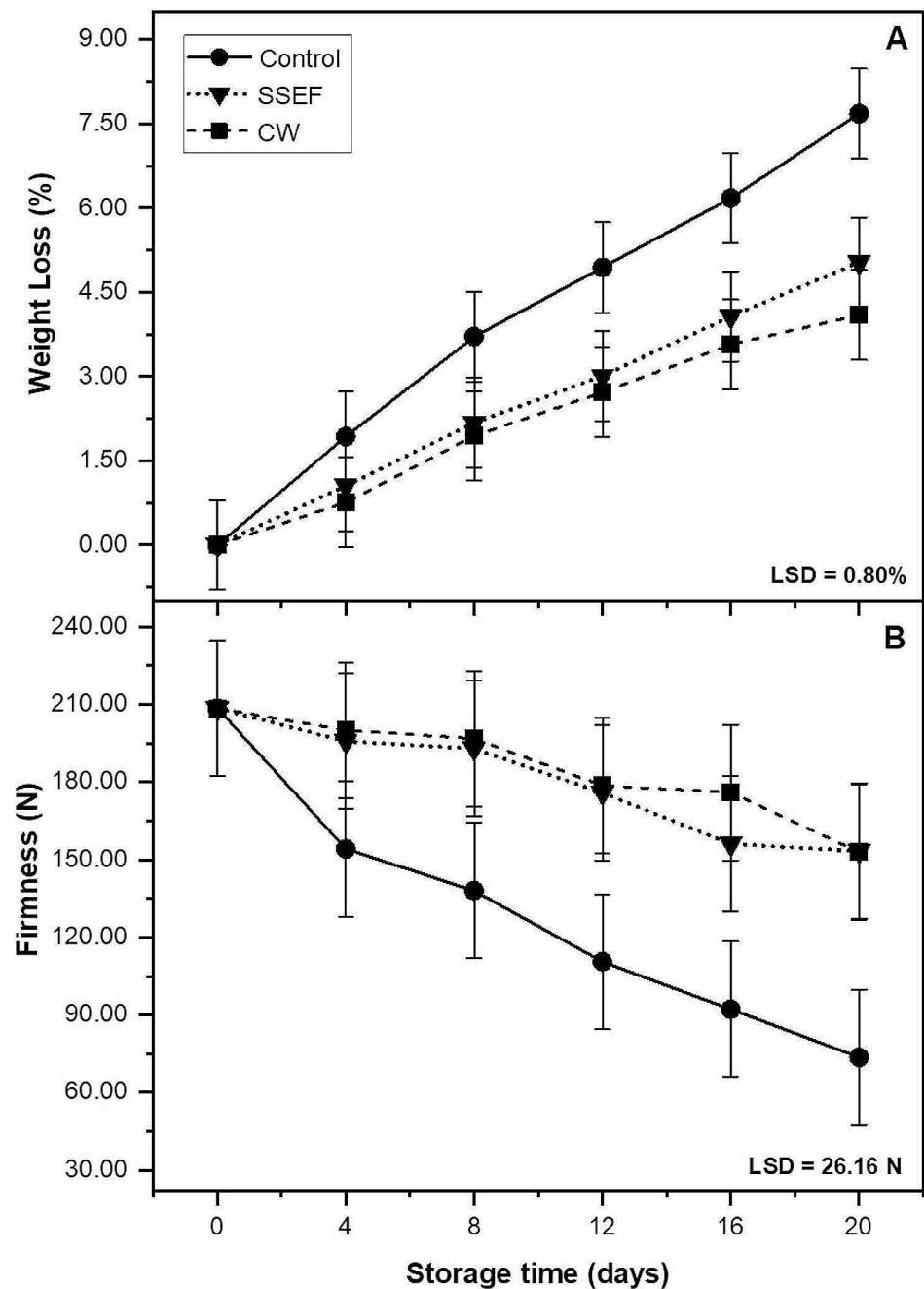
Firmness

Fruit tissue firmness is a critical physical factor determining its quality and acceptability. As shown in Fig. 4b, all treatments lost firmness regarding the storage time. In control fruits, the firmness decreased from 204.55 ± 16.61 N to 73.56 ± 31.46 N, showing a significant difference ($P < 0.05$) regarding SSEF and CW after day 8 of storage. Calderón-Castro et al. [15] and Fitch-Vargas et al. [17] reported that ripening reduces fruit

firmness, promoting the cell wall components' breakdown, such as pectins, through enzymes like polygalacturonase and pectin-methylesterase. As a result, ripening reduces intracellular adhesiveness and tissue stiffness, converting carbohydrates into simpler units and water loss through transpiration.

SSEF and CW exhibited similar behavior throughout the storage with no significant difference ($P > 0.05$), recording final values of 153.34 ± 32.15 N and 153.00 ± 23.65 N, respectively. It is well known that CW is particularly effective in delaying ripening due to its ability to create a barrier that reduces fruit's transpiration [44]. Likewise, SSEF could have inhibited the ethylene production induced by increased CO_2 levels and reduced O_2 levels within the internal fruit atmosphere, resulting in a decline in pectinesterase and polygalacturonase enzymatic activity [17]. This possible inhibition may be related to the formation of hydrogen bonds between the polymer matrix and the mango surface, resulting in good adhesion and the formation of a solid and cohesive layer that prevents water loss and creates a suitable atmosphere for the fruit. López et al. [33] recorded a decrease in WVP in succinate starch-based films due to the hydrophobic substituent group. This behavior coincides with

Fig. 4 Weight loss (**a**) and firmness (**b**) of mangoes cv. Kent stored for 20 days at 12 ± 1 °C. Vertical bars indicate LSD ($P < 0.05$)



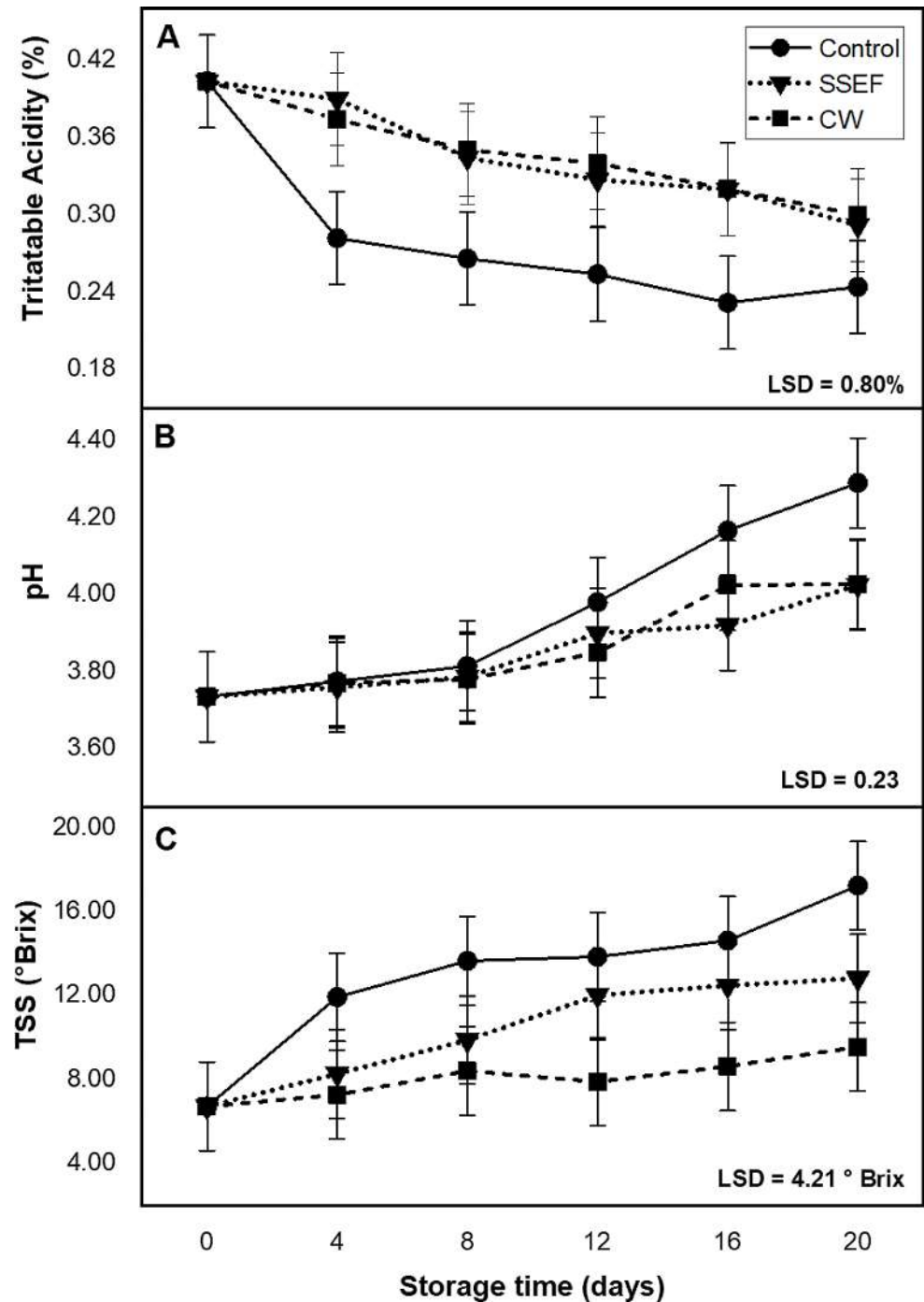
the outcomes of this research, where a hydrophobic coating reduces the fruit's water transfer and firmness.

Titrateable acidity

Titrateable acidity (TA) measures the total amount of organic acids present in food, and its reduction during fruit ripening indicates an acceleration in the respiration process [45]. Figure 5a shows that TA decreased for all

treatments through 20 days of storage at 12 ± 1 °C. The control exhibited the lowest TA values throughout the essay, recording a significant difference ($P < 0.05$) from day 4 to 16 compared to coated fruits. On day 20, no significant difference ($P > 0.05$) among treatments was recorded. On the other hand, SSEF did not record a significant difference ($P > 0.05$) with CW during the assessment period. It is well known that coatings can delay the fruit's ripening process by creating a barrier to gas

Fig. 5 Titratable Acidity (a), pH (b), and total soluble solids (c) of mangoes cv. Kent stored for 20 days at 12 ± 1 °C. Vertical bars indicate LSD ($P < 0.05$)



diffusion, modifying its atmosphere. These alterations can lead to a reduction in the respiration rate and avoid the consumption of acid organics [32, 44]. In the context of starch-based films, the presence of amylose and amylopectin suggests the existence of both amorphous and crystalline regions, facilitating the selective permeability of certain gases [45]. However, for this barrier to form, there must be a good interaction between the

coating and the fruit surface, coupled with favorable storage conditions.

pH

Figure 5b illustrates pH results for all treatments over 20 days of storage at 12 ± 1 °C. As the fruit ripens, the pH increases, a change associated with the biochemical reactions during cellular respiration. These reactions facilitate

the conversion of organic acids into sugars [46, 47]. Control registered the highest pH values throughout the essay, reaching a final value of 4.39 ± 0.24 and presenting a significant difference ($P < 0.05$) regarding SSEF and CW on day 20. On the other hand, SSEF and CW recorded lower final values of pH, 4.02 ± 0.20 and 4.00 ± 0.36 , respectively. This reduction may be related to the effect generated by the coating, which would help to inhibit metabolic activity and, therefore, the conversion of organic acids to sugars [47]. Restrepo and Aristizábal [48] observed lower pH in strawberries covered with carnauba wax and aloe vera untreated strawberries. Moreira et al. [47] reported reduced pH in guava fruits covered by modified starch and gelatin compared to uncovered fruits.

Total soluble solids (TSS)

The TSS are water-soluble fruit components, including sugars, vitamins, amino acids, and some pectin. As the

fruit ripens, the acidity decreases, resulting in a sweeter fruit [4]. All the treatments showed an increase in TSS over a 20-day storage period (Fig. 5c). Control recorded a final value of 17.2 °Brix, while SSEF and CW exhibited lower TSS values (12.8 ± 0.23 °Brix and 9.54 ± 1.56 °Brix, respectively). Coatings may reduce both respiratory and enzymatic activities, which are responsible for the hydrolysis of starches into simpler sugars [49]. The effect of SSEF on mango may be attributed to the reduced gas diffusion due to the presence of modified starch, creating a more compact network [27, 50]. Moreira et al. [47] reported that the modified starch and gelatin-based coating on guava reduced the TSS to 15 days after harvest.

Conclusions

Edible films based on succinylated corn starch were successfully produced for subsequent application as coatings on mango fruits. Regarding the study factors of the experimental design, the DS had a significant effect ($P < 0.01$) on all the response variables when it increased, promoting a decrease in S, WVP, and CO_2P and an increase in PS. From the numerical optimization, it was obtained that the best conditions to obtain edible films with good mechanical and barrier properties were $\text{DS} = 0.05$ and $\text{GC} = 19.85\%$. On the other hand, the microstructural analyses helped confirm the chemical modification in the succinylated starch and the presence of succinyl groups in the optimized edible film. Finally, the mango fruits coated with the optimal formulation maintained their postharvest quality during 20 days of storage at 12 °C, registering better or similar values to carnauba wax.

Therefore, succinylated starch-based coatings could help maintain postharvest quality and extend the shelf life of mango cv. Kent.

Although the development of films and edible coatings based on extrusion-reactive modified starch represents an environmentally friendly option for obtaining bioplastics that can extend the shelf life of perishable foods, it is crucial to acknowledge the inherent limitations and opportunity areas within our study. In the process of obtaining modified starch and the coating-forming solution, it is essential to optimize the processing conditions and address challenges associated with industrial-scale implementation to achieve improved performance and ensure economic viability.

Future research should focus on exploring new sources of starch, as well as improving the controlled release of active ingredients to enhance the functionality of edible coatings. On the other hand, it is known that some drawbacks of starch-based coatings are their poor barrier properties. Therefore, exploring combinations with other raw materials or making use of nanotechnology is imperative to enhance the primary function of these materials, which is to maintain quality and prolong the shelf life of fruits and vegetables. Consequently, it is vital to continue research on multiple fronts to improve the effectiveness and applicability of starch-based coatings at an industrial level.

Acknowledgements The authors thank CONACYT for supplying financial support for developing this work and Dr. Fernando Martínez-Bustos from CINVESTAV Querétaro for providing support to carry out the microstructural analyses.

Author contributions P.R. Fitch-Vargas designed the experiment, prepared the manuscript, and interpreted the results. E. Aguilar-Palazuelos conducted all the experiments and analyzed the data. X.A. Ruiz-Armenta, C. Barraza-Elenes, and C.I. Delgado-Nieblas revised the manuscript and provided technical support. A. Calderón-Castro supervised the entire experiment and contributed to manuscript preparation.

Funding Not applicable.

Data availability Not applicable.

Declarations

Competing interest The authors declare no competing interests. The manuscript has not been submitted for publication in other media with substantial circulation. All previously published works cited in the manuscript have been duly acknowledged. All authors have made substantial contributions to the manuscript and approved the final submission. No interest conflicts exist between the authors and the reviewers who assessed this manuscript. The preparation of this manuscript strictly adhered to the journal formatting provided in the authors' guide.

References

1. M. Kurtfaki, M.J. Yildirim-Yalcin, *Food Meas. Charact.* **1–9** (2023). <https://doi.org/10.1007/s11694-023-02013-4>
2. N. Noshirvani, I. Alimari, H.J. Mantashloo, *Food Meas. Charact.* **17**(5), 5440–5454 (2023). <https://doi.org/10.1007/s11694-023-02048-7>
3. A.M. Ribeiro, B.N. Estevinho, F. Rocha, *Food Bioprocess. Technol.* **14**, 209–231 (2021). <https://doi.org/10.1007/s11947-020-02528-4>
4. T.J. Gutiérrez, N.J. Morales, M.S. Tapia, E. Pérez, L. Famá, *Procedia Mater. Sci.* **8**, 304–310 (2015). <https://doi.org/10.1016/j.mspro.2015.04.077>
5. J. Li, F. Ye, J. Liu, G. Zhao, *Food Hydrocoll.* **46**, 226–232 (2015). <https://doi.org/10.1016/j.foodhyd.2014.12.017>
6. M.C. Cortez-Trejo, A. Wall-Medrano, M. Gaytán-Martínez, S. Mendoza, *Food Biosci.* **41**, 100929 (2021). <https://doi.org/10.1016/j.foodbi.2021.100929>
7. L.Z. Jaekel, M. Schmiele, R. da Silva Rodrigues, Y.K. Chang, *J. Food Sci. Technol.* **52**, 7305–7312 (2015). <https://doi.org/10.1007/s13197-015-1804-5>
8. M.V. Tupa, J.A.A. Ramírez, A. Vázquez, M.L. Foresti, *Food Chem.* **170**, 295–302 (2015). <https://doi.org/10.1016/j.foodchem.2014.08.062>
9. S. Punia, K.S. Sandhu, S.B. Dhull, M. Kaur, *Int. J. Biol. Macromol.* **133**, 110–116 (2019). <https://doi.org/10.1016/j.ijbiomac.2019.04.089>
10. A. Rincón-Aguirre, L.A. Bello Pérez, S. Mendoza, A. del Real, M.E. Rodríguez García, *Starch-Stärke*, **70**(3–4), 1700066 (2018). <https://doi.org/10.1002/star.201700066>
11. Z. Liu, X. Liu, Y. Cao, W. Xie, X.X.J. Ma, *Yu Appl. Polym. Sci.* **127**(4), 2922–2927 (2013). <https://doi.org/10.1002/app.37773>
12. P.V.F. Lemos, H.R. Marcelino, L.G. Cardoso, C.O. de Souza, J.I. Druzian, *Int. J. Biol. Macromol.* **184**, 218–234 (2021). <https://doi.org/10.1016/j.ijbiomac.2021.06.077>
13. A. Calderón-Castro, N. Jacobo-Valenzuela, L.A. Félix-Salazar, J.D.J. Zazueta-Morales, F. Martínez-Bustos, P.R. Fitch-Vargas, E. Aguilar-Palazuelos, *J. Food Sci. Technol.* **56**, 3940–3950 (2019). <https://doi.org/10.1007/s13197-019-03863-x>
14. J. Xu, T.D. Andrews, Y.C. Shi, *Starch-Stärke*, **72**(3–4) (2020). 1900238 <https://doi.org/10.1002/star.201900238>
15. A. Calderón-Castro, M.O. Vega-García, J.J. Zazueta-Morales, P.R. Fitch-Vargas, A. Carrillo-López, R. Gutiérrez-Dorado, E. Aguilar-Palazuelos, *Food Sci. Technol.* **55**, 905–914 (2018). <https://doi.org/10.1007/s13197-017-2997-6>
16. X. Wang, L. Huang, C. Zhang, Y. Deng, P. Xie, L. Liu, J. Cheng, *Carbohydr. Polym.* **240**, 116292 (2020). <https://doi.org/10.1016/j.carbpol.2020.116292>
17. P.R. Fitch-Vargas, E. Aguilar-Palazuelos, J.J. Zazueta-Morales, M.O. Vega-García, J.E. Valdez-Morales, F. Martínez-Bustos, N. Jacobo-Valenzuela, *J. Food Sci.* **81**(9), E2224–E2232 (2016). <https://doi.org/10.1111/1750-3841.13416>
18. E. Ayranci, S. Tunc, *Food Chem.* **72**(2), 231–236 (2001). [https://doi.org/10.1016/S0308-8146\(00\)00227-2](https://doi.org/10.1016/S0308-8146(00)00227-2)
19. M. Chiumarelli, M.D. Hubinger, *Food Hydrocoll.* **38**, 20–27 (2014). <https://doi.org/10.1016/j.foodhyd.2013.11.013>
20. W. Zhou, J. Lian, J. Zhang, Z. Mei, Y. Gao, G. Hui, *Food Meas. Charact.* **1–11** (2023). <https://doi.org/10.1007/s11694-023-01865-0>
21. AOAC, *Official Methods of Analysis*, 19th edn. (Association of Official Analytical Chemists Inc, Arlington, 2012)
22. L.X. Zhong, X.W. Peng, D. Yang, X.F. Cao, R.C. Sun, *J. Agric. Food Chem.* **61**(3), 655–661 (2013). <https://doi.org/10.1021/jf304818f>
23. L. Ren, Q. Wang, X. Yan, J. Tong, J. Zhou, X. Su, *Food Res. Int.* **87**, 180–188 (2016). <https://doi.org/10.1016/j.foodres.2016.07.007>
24. U. Shah, F. Naqash, A. Gani, F.A. Masoodi, *Compr. Rev. Food Sci. Food Saf.* **15**(3), 568–580 (2016). <https://doi.org/10.1111/1541-4337.12197>
25. A. Escalante, A. Gonçalves, A.A. Bodin, C. Stepan, G. Sandström, P. Toriz, Gatenholm, *Carbohydr. Polym.* **87**(4), 2381–2387 (2012). <https://doi.org/10.1016/j.carbpol.2011.11.003>
26. A.B. Dias, C.M. Müller, F.D. Larotonda, J.B. Laurindo, *J. Cereal Sci.* **51**(2), 213–219 (2010). <https://doi.org/10.1016/j.jcs.2009.11.014>
27. L. Qiu, F. Hu, Y. Peng, *Carbohydr. Polym.* **91**(2), 590–596 (2013). <https://doi.org/10.1016/j.carbpol.2012.08.072>
28. M.A. Cerqueira, B.W. Souza, J.A. Teixeira, A.A. Vicente, *Food Bioprocess. Technol.* **6**, 1600–1608 (2013). <https://doi.org/10.1007/s11947-011-0753-x>
29. A. Pérez-Gallardo, L.A. Bello-Pérez, B. García-Almendárez, G. Montejano-Gaitán, G. Barbosa-Cánovas, C. Regalado, *Starch-Stärke*, **64**(1), 27–36 (2012). <https://doi.org/10.1002/star.201100042>
30. J. Zhou, L. Ren, J. Tong, L. Xie, Z. Liu, *Carbohydr. Polym.* **78**(4), 888–893 (2009). <https://doi.org/10.1016/j.carbpol.2009.07.017>
31. H.H. Gahruie, M.H. Eskandari, P. Van der Meer, S.M.H. Hosseini, *Carbohydr. Polym.* **219**, 155–161 (2019)
32. M.A. Aguilar-Méndez, E.S. Martín-Martínez, S.A. Tomas, A. Cruz-Orea, M.R. Jaime-Fonseca, *J. Sci. Food Agric.* **88**(2), 185–193 (2008). <https://doi.org/10.1002/jsfa.3068>
33. O.V. López, N.E. Zaritzky, M.V. Grossmann, M.A. García, *J. Food Eng.* **116**(2), 286–297 (2013). <https://doi.org/10.1016/j.jfoodeng.2012.12.032>
34. K. Wang, W. Wang, R. Ye, A. Liu, J. Xiao, Y. Liu, Y. Zhao, *Food Chem.* **216**, 209–216 (2017). <https://doi.org/10.1016/j.foodchem.2016.08.048>
35. Y. Kim, H.B. Lamsal, J.L. Jane, D. Grewell, *J. Food Process. Eng.* **43**(3) (2020). <https://doi.org/10.1111/jfpe.13216>
36. M. Lopez-Silva, E. Agama-Acevedo, L.A. Bello-Perez, J. Alvarez-Ramirez, *Carbohydr. Polym.* **270**, 118378 (2021). <https://doi.org/10.1016/j.carbpol.2021.118378>
37. D. Wu, Q. Lin, H. Singh, A. Ye, *Food Res. Int.* **136**, 109350 (2020). <https://doi.org/10.1016/j.foodres.2020.109350>
38. U.A. Basilio-Cortés, L. González-Cruz, G. Velázquez, G. Teniente-Martínez, C.A. Gómez-Aldapa, J. Castro-Rosas, A. Bernardino-Nicanor, *Polymers*, **11**(2), 333 (2019). <https://doi.org/10.3390/polym11020333>
39. S. Jiang, L. Dai, Y. Qin, L. Xiong, Q. Sun, *PloS One*, **11**(2) (2016). <https://doi.org/10.1371/journal.pone.0150043>
40. F. Cruces, M.G. García, N.A. Ochoa, *Food Bioprocess. Technol.* **14**(7), 1244–1255 (2021). <https://doi.org/10.1007/s11947-021-02628-9>
41. A. Kocira, K. Kozłowiec, K. Panasiewicz, M. Staniak, E. Szpunar-Krok, P. Horyńska, *Agron.* **11**(5), 813 (2021). <https://doi.org/10.3390/agronomy11050813>
42. G. Hui, W. Liu, H. Feng, J. Li, Y. Gao, *Food Chem.* **203**, 276–282 (2016). <https://doi.org/10.1016/j.foodchem.2016.01.12>
43. J. Peng, F. Zheng, L. Wei, H. Lin, J. Jiang, G. Hui, *Food Meas. Charact.* **12**(1), 78–86 (2017). <https://doi.org/10.1007/s11694-017-9618-y>
44. H. Chen, Z. Sun, H. Yang, *Sci. Hortic.* **244**, 157–164 (2019). <https://doi.org/10.1016/j.scienta.2018.09.039>
45. H.-G. Song, I. Choi, J.-S. Lee, M.-N. Chung, C.S. Yoon, J. Han, *Int. J. Biol. Macromol.* **189**, 758–767 (2021). <https://doi.org/10.1016/j.ijbiomac.2021.08.106>
46. K. Dulta, G. Koşarsoy Ağçeli, A. Thakur, S. Singh, P. Chauhan, P.K. Chauhan, *J. Polym. Environ.* **30**(8), 3293–3306 (2022). <https://doi.org/10.1007/s10924-022-02411-7>

47. E.D.S. Moreira, N.M.C.D. Silva, M.R.S. Brandão, H.C. Santos, T.A.P.D.C. Ferreira, *Food Sci. Technol.* **42**, e26221 (2021). <https://doi.org/10.1590/fst.26221>
48. J.I. Restrepo, I.D. Aristizábal, *Vitae*. **17**(3), 252–263 (2010)
49. M.S. Saleem, S. Ejaz, M.A. Anjum, A. Nawaz, S. Naz, S. Husain, I. Canan, J. *Food Process. Preserv.* **44**(8) (2020). <https://doi.org/10.1111/jfpp.14583>. e14583
50. A.J. Vellaisamy Singaram, S. Guruchandran, A. Bakshi, C. Muniathan, N.D. Ganesan, *Packag Technol. Sci.* **34**(8), 485–495 (2021). <https://doi.org/10.1002/pts.2574>

Publisher's Note Springer Nature remains neutral with regard to jurisdictional claims in published maps and institutional affiliations.

Springer Nature or its licensor (e.g. a society or other partner) holds exclusive rights to this article under a publishing agreement with the author(s) or other rightsholder(s); author self-archiving of the accepted manuscript version of this article is solely governed by the terms of such publishing agreement and applicable law.